

TIME-RESOLVED FLUORESCENCE MEASUREMENTS FOR THE CHARACTERIZATION OF EPOXY SYSTEMS

B. STREHMEL,* V. STREHMEL, H.-J. TIMPE and K. URBAN

Chemistry Department, Technical University Merseburg, 4200 Merseburg, Fed. Rep. Germany

(Received 30 July 1991)

Abstract—Time-resolved fluorescence measurements, with Methyl Violet as probe, were used to determine some microviscosity and free volume parameters in the diglycidylether of bisphenol-A, in novolacs derived from bisphenol-A and in their mixtures. The fluorescence of the probe must compete with an internal rotational process of parts of the molecule. Due to the influence of surroundings on that process, the fluorescence lifetimes are related to mobilities in the system. Using known theoretical approaches for describing the mobility parameters in polymers or high-viscosity media, relations between the rate constant for the probe rotational and these parameters have been derived. With combined time-resolved fluorescence, viscosity-dependent and temperature-dependent measurements, fractional free volume data and glass transition temperatures have been determined. In novolac-diglycidyl ether mixtures, evidence for strong hydrogen bondings has been found.

INTRODUCTION

Epoxy resins are important materials because of properties such as high temperature performance, solvent resistance, good adhesion to metal surfaces and favourable electrical and mechanical behaviour. Today, epoxies are used for high performance composites [1], as adhesives [2], for manufacturing of various electronic devices [3] and printing plates [4]. For such applications, materials are formed by curing of low-molecular compounds containing the epoxide group with hardeners, finally yielding networks. The mentioned properties of the materials strongly depend on the network formation process. Therefore, deeper understanding of this process and the network structure is required.

Among the methods capable of providing the required information, those based on photophysical principles are important [5-8]. Microscopic parameters so obtained are more suitable for describing the diffusion controlled crosslinking reactions than the normal macroscopic values.

So far, the following procedures have been used for the characterization of epoxy compounds:

- (1) direct fluorescence of epoxies [9];
- (2) fluorescence spectroscopy with excimer-forming probes [10];
- (3) fluorescence anisotropy measurements [11, 12].

Normally, intensity-derived signals of the emitting species are used for calculations but the fluorescence method is restricted to special cases [13].

We now report experimental studies on lifetimes of a fluorescence probe in an unhardened epoxy system with time-correlated single photon counting (TC-SPC). It was the aim to find correlations between lifetime-derived parameters and microviscosity, free

volume parameters and molecular mobility of the system. The diglycidylether of bisphenol-A (DGEBA) and novolacs derived from bisphenol-A (DNL) served as model compounds (see Scheme 1). Methyl Violet (MV) was used as fluorescence probe.

EXPERIMENTAL PROCEDURES

The epoxy compound DGEBA (Leuna-Werke AG) was recrystallized twice from methanol, m.p. 44°. Methyl Violet (Aldrich) was used as received without further purification. The novolacs based on bisphenol-A were synthesized as already described [14] by condensation of bisphenol-A and formaldehyde provided by a formaldehyde precursor at 200°C. The resins were characterized by ¹H-NMR, ¹³C-NMR, i.r. and HPLC [14].

Determination of molecular weights

The number-average molecular weights (\bar{M}_n) of novolacs have been determined using a vapour pressure osmometer 11.00 (Fa. Knauer) at 70°C. Methyl ethyl ketone served as solvent for all compounds and dibenzoyl as standard.

Differential scanning calorimetry

All glass transition temperatures (T_g) were determined using DSC-7 equipment (Perkin-Elmer). Before the determination the samples were run at a heating rate of 20°C min⁻¹. The T_g values were determined with second scans at a heating rate of 10°C min⁻¹.

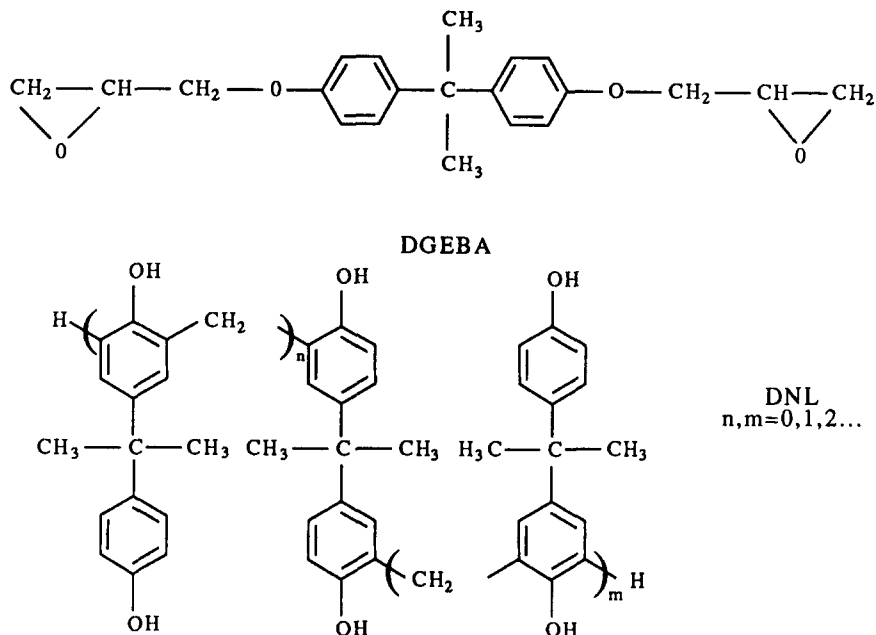
Viscosity measurements

The viscosities of DGEBA between 30 and 70°C were measured with a Höppler viscometer. Glycerol, for which the temperature dependence of viscosity is known [15], was used as standard.

Time-correlated single photon counting set up

The equipment is illustrated in Fig. 1. An argon ion laser ILA 120-1 (Carl Zeiss Jena AG) was used as light source. In combination with a modulator (M) and an acousto-optical modulator (AOM) (Friedrich Schiller University Jena), this laser produces periodical impulses with lifetimes of ca 85 psec and frequencies of 123.2 MHz. In part, the light goes

*To whom all correspondence should be addressed.



Scheme 1

through a Brewster prism to a photodiode SP 102, which directly measures the laser light intensity. Part of the light reaches an Avelange photodiode BPW 28 A (Telefunken AG) and is used to provide trigger signals. Another part of the laser light goes through the optical system to the probe contained in a spectroscopic cell. The emitted fluorescence light of the probe is measured with a Specord monochromator (Carl Zeiss Jena AG) and a photomultiplier (SEV) TUV 5502 (Valvo). The SEV transfers the registered photon impulse to the single photon counting system (SPC). Data thus obtained can be plotted with a X-Y recorder. The SPC is coupled with a PC AT 286/20 (Fa. Wilmy).

Deconvolutions necessary for experimental signals were made using the phase plane method or Marquardt's non-linear calculation algorithm. The SPC system was calibrated

with 10^{-5} M solutions of pinacyanol (Lambda Physics) in methanol. The lifetime of pinacyanol lies between 5 to 10 psec. With the set-up described, the time resolution is > 30 psec.

Probe preparations

The experiments with pure DGEBA and mixtures of DGEBA with novolacs were carried out in 1 mm cells at an angle of 45° . The fluorescence light was detected at the magic angle (54.7°). Novolacs were measured as thin films (thickness *ca* $5 \mu\text{m}$). The films were prepared by coating 5 wt% solution of novolacs in acetone containing 10^{-3} M MV on polyester sheets (thickness *ca* $500 \mu\text{m}$). Films thus obtained were dried at room temperature for 24 hr in the dark.

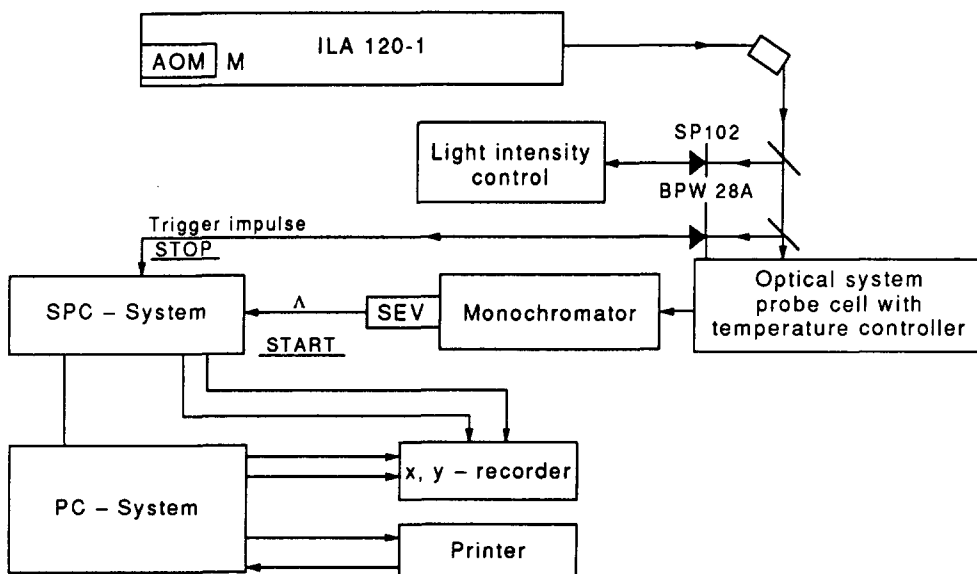
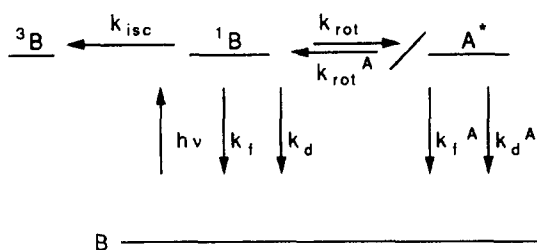


Fig. 1. Construction scheme of the set up for time-correlated single photon counting measurements (abbreviations see Experimental procedures).



Scheme 2. Photochemical pathways of fluorescence probes.

RESULTS AND DISCUSSION

Selection of the fluorescence probe

A compound, to be used as fluorescence probe for time-correlated single photon counting measurements, must possess the following general properties:

- inertness against the substances contained in the system and the reactions carried out;
- quantitative solubility in the system;
- selective absorption of the incident light;
- viscosity-dependent fluorescence.

Of these requirements, the last is the most important if the aforementioned problems are to be investigated. In Scheme 2, a general example is given for a substance (B), which satisfies this prerequisite.

After excitation, the excited species (¹B) deactivates either radiatively (k_r) or non-radiatively (k_d) to its

ground state (B), or yields via isc-process (k_{isc}) its triplet state (³B), or forms via the rotation process (k_{rot}) the excited species A*. Thus, a conformer of ¹B, more energetically stable, will be formed, which is in principle also capable of emitting light (k_r^A) but that emission is very weak because the rotational process $A^* \rightarrow B$ is symmetrically forbidden [16]. Therefore, the light emitted from ¹B is not influenced by another emission process. It is important to note that only the rotation of parts of the molecule in ¹B and A* is viscosity dependent.

Photochemical pathways shown in Scheme 2 are already known [16–19]. Triphenylmethane dyes have been described as compounds possessing strongly viscosity-dependent fluorescence [17–19]. Therefore, we used MV as fluorescence probe for polymers. This compound satisfies the stated main prerequisites for a fluorescence probe; see Fig. 2. The excited state ¹B of MV is very short-lived in fluid media [16]. Thus, dynamic time-resolved measurements must be used to analyse the polymeric system. Further, the rotational process of ¹B in MV does not possess an intramolecular barrier.

So, lifetime (τ_r) measurements of the excited state ¹B give direct information about the elementary processes of the probe in the polymeric matrix. Because these processes are very fast (10^{-9} – 10^{-12} sec), they are influenced less by those surroundings, the exception of the rotational process. However, the latter is restricted by change in viscosity in

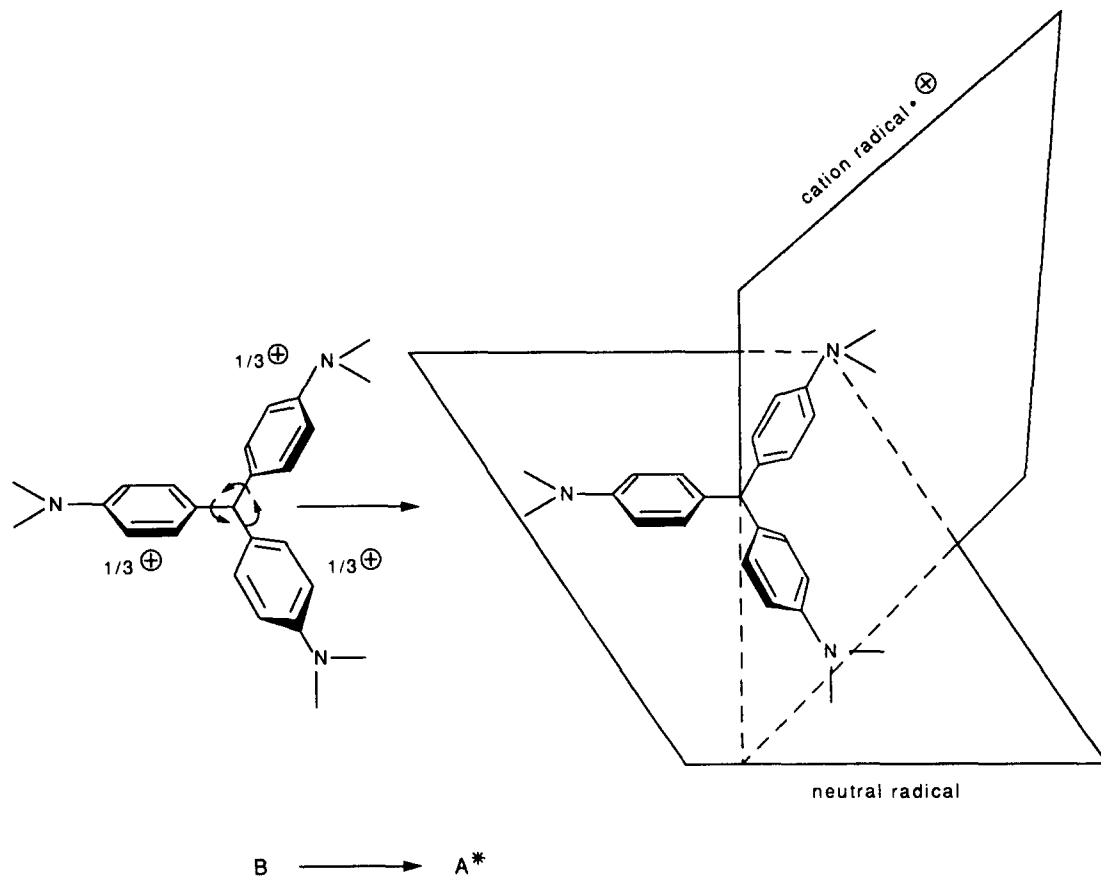


Fig. 2. Structures of species B and A* of the fluorescence probe MV.

the direct neighbourhood of the probe molecule. To a first approximation, the excited probe molecule does not interact dynamically within its short lifetime with the surrounding macromolecules or with parts of these molecules. The τ_f values can be calculated from the primary experimental results (see typical example in Fig. 3; the number of channels is a mean for the delay time) using:

$$I_f(t) \sim \exp(-t/\tau_f) \quad (1)$$

where $I_f(t)$ is the emitted light intensity at time t . The mathematical procedures necessary for τ_f calculations are given in the experimental part.

Corresponding to Scheme 2, τ_f can be expressed by:

$$\tau_f = \frac{1}{k_f + k_d + k_{isc} + k_q[Q] + k_{rot}} \quad (2)$$

where $k_q[Q]$ is the rate of quenching by an external quencher. For calculations of k_{rot} , the value of the sum ($k_f + k_d + k_{isc} + k_q[Q]$) must be known. This parameter is given by:

$$\tau_f^0 = \frac{1}{k_f + k_d + k_{isc} + k_q[Q]} \quad (3)$$

From equations (2) and (3)

$$k_{rot} = \frac{1}{\tau_f} - \frac{1}{\tau_f^0} = \frac{1}{\tau_{rot}} \quad (4)$$

Because the rotation process is based on first order kinetics, the rotational lifetime (τ_{rot}) of the probe can also be used to express quantitatively the process. Furthermore, for linear plots of k_{rot} or τ_{rot} against a varied parameter, the experimental value τ_f can be employed.

In fluid systems, the rotational process is the fastest of all the deactivation processes of 1B . If this process is restricted, then the τ_f or τ_{rot} values are increased. Thus, changes of τ_f indicate changes of the rotational mobility of the probe molecule in the polymeric matrix. An increased τ_f is caused by stronger hindrances to probe rotational process caused by the surroundings. In this case, k_{rot} decreases and therefore τ_f approaches the value of τ_f^0 . This value for MV is given by $\tau_f^0 = 4$ nsec [20].

It is necessary to verify that, in the delay time period chosen, only one emitting process occurs. This prerequisite is an important requirement for easy application of the discussed method. As can be seen from Fig. 4, over the whole delay period, with MV the same fluorescence spectrum has been obtained. Both, shape and position of this spectrum match in all details those found for solutions of MV in low molecular solvents.

Further, as follows from equations (3) and (4), the parameter $k_q(Q)$ also must be independent of changes in the polymeric surroundings. Due to the very small lifetime τ_f^0 , the value of that parameter must lie between 10^8 and 10^9 sec $^{-1}$ to influence significantly the lifetime of 1B . Because k_q can reach only the diffusion-controlled limit, then the quencher concentration must be in the molar region. In the given system, such a concentration can be reached by the polymer itself and therefore the polymeric matrix does not itself react as a quencher.

The selected MV probe possesses some advantages over other proposed probes. In the case of azo dyes [21, 22], E-Z isomerization is responsible for the viscosity-dependent process; this isomerization can follow either a rotation or an inversion mechanism.

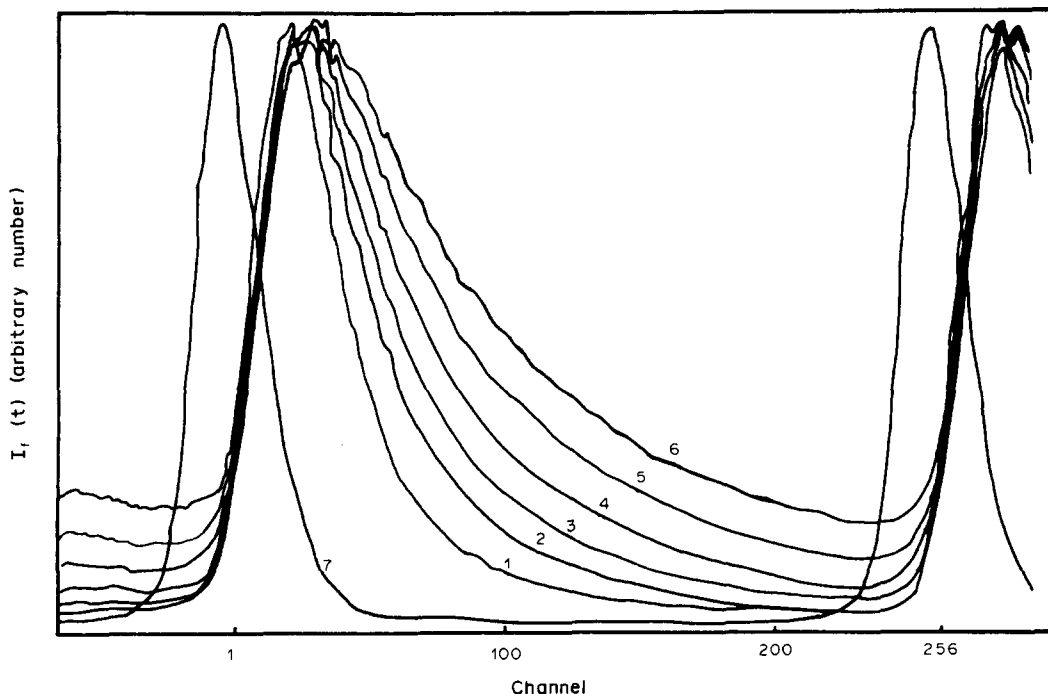


Fig. 3. Fluorescence decay curves of MV in a mixture of 3 g DGEBA and 2.5 g DNL at various temperatures. 1, 283 K; 2, 293 K; 3, 303 K; 4, 313 K; 5, 323 K; 6, 333 K; 7, delay curve of laser flash (excitation with $\lambda^{ex} = 514$ nm, registration at $\lambda^{em} = 640$ nm).

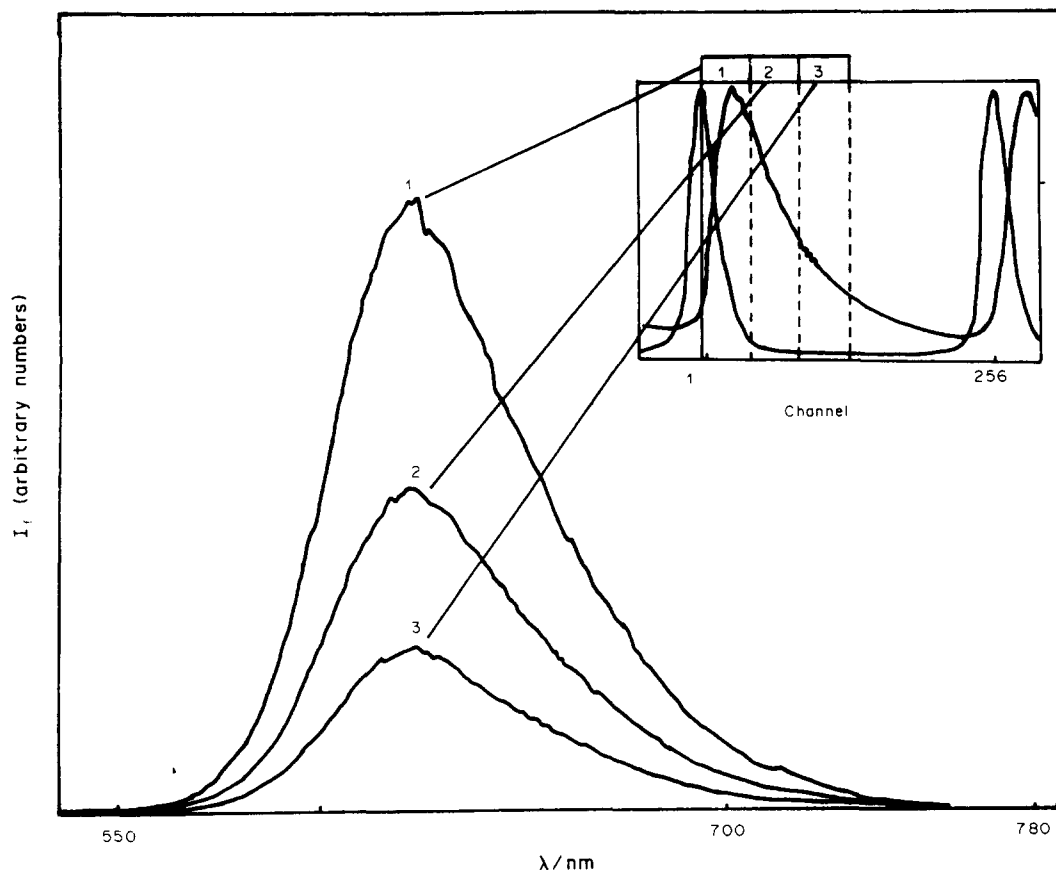


Fig. 4. Fluorescence spectra of MV at various times after the flash (experimental conditions as for Fig. 3).

So it is unclear which reaction volume is necessary for the viscosity-dependent rotation process [23]. Further, sometimes both geometric isomers of azo dyes give fluorescence signals difficult to analyse.

Relations between probe fluorescence derived parameters and viscosity-dependent parameters

For describing the viscosity-dependent processes, there are three fundamental treatments, viz. Debye-Stokes-Einstein (DSE) theory [24], Eyrings hole-theory [25] and the microviscosity theory of Gierer and Wirtz [26]. For the systems investigated here, the last model should be the most useful. Therefore, the following expression holds between macroscopic viscosity (η) and k_{rot} [27]

$$k_{\text{rot}}\eta = \alpha + \delta\eta^\gamma \quad (5)$$

where α is the DSE factor and δ is the microviscosity factor derived from the probe used. The exponent γ is a measure of the portion of the rotation of "solvated" probe molecule into "holes" of the polymeric matrix. It is given by:

$$\gamma = \frac{E_a^{\text{dv}} - E_a^{\text{mv}}}{E_a^{\text{dv}}} \quad (6)$$

where E_a^{dv} is the activation energy of the rotational process derived from dynamic viscosity, E_a^{mv} is the activation energy of rotational process derived from microviscosity.

The value of E_a^{dv} can be determined experimentally by measuring η as a function of temperature (T):

$$\eta = \eta_0 \exp(E_a^{\text{dv}}/RT) \quad (7)$$

with η_0 being the viscosity at infinite temperature.

This process corresponds to Stokes rotational diffusion.

In general, the rotational mobility (m_{rot}) of the probe in a polymeric system is given by [28]:

$$m_{\text{rot}} = A \exp(-V'_{\text{cr}}/HV'_f) \quad (8)$$

where A is the pre-exponential coefficient, V'_{cr} is the fractional critical free volume, V'_f is the fractional free volume. Using the experimental values of k_{rot} or τ_{rot} one obtains

$$k_{\text{rot}} = k_{\text{rot}}^0 \exp(-V'_{\text{cr}}/V'_f) \quad (9)$$

$$\tau_{\text{rot}} = \tau_{\text{rot}}^0 \exp(V'_{\text{cr}}/V'_f) \quad (10)$$

with the known expression

$$V'_{\text{cr}} = (\beta V_0)' \quad (11)$$

equation (10) is transformed to

$$\tau_{\text{rot}} = \tau_{\text{rot}}^0 \exp((\beta V_0)'/V'_f) \quad (12)$$

with V_0 being the volume swept out by the rotating group of the probe molecule (approximately identical with its van der Waals volume).

As follows from equation (10), the ratio of the critical free volume to the free volume of the polymeric matrix determines the rotational mobility of the

probe. Further, the temperature dependence of τ_{rot} can be expressed by

$$\tau_{\text{rot}} = \tau_{\text{rot}}^0 \exp(E_a^{\text{rot}}/RT) \quad (13)$$

where E_a^{rot} is the activation energy of the rotational process of the probe.

Because there are internal rotation barriers in the probe molecule, measured E_a^{rot} values express the hindrance to the rotation of probe molecules by the polymeric matrix. Equation (12) can be used for polymer systems below and above T_g but the values of E_a^{rot} are different for the two regions. Therefore, from the crossing points of appropriate Arrhenius plots, values of T_g can be determined.

Substituting τ_{rot} in equation (13) by equation (12) results in:

$$\frac{E_a^{\text{rot}}}{RT} = \frac{(\beta V_0)'}{V_f'} \quad (14)$$

From the above parameters, the fractional free volume can be calculated with equation (15), which is derived from the WLF-theory [29] and is obeyed above T_g .

$$V_f' = V_f^\ddagger + \alpha_f(T - T_g) \quad (15)$$

where V_f^\ddagger is the fractional free volume at T_g ($V_f^\ddagger = 0.025$) [29, 30], α_f is the thermal expansion coefficient ($\alpha_f = 4.8 \cdot 10^{-4} \text{ K}^{-1}$ [29, 30]).

Using equation (16), V_f' can be determined also from temperature dependent measurements of the macroscopic viscosity [31].

$$\ln \eta = \ln \eta^\ddagger - \frac{\alpha_f(T - T_g)}{[V_f^\ddagger + \alpha_f(T - T_g)]V_f^\ddagger} \quad (16)$$

with η^\ddagger being the viscosity at T_g .

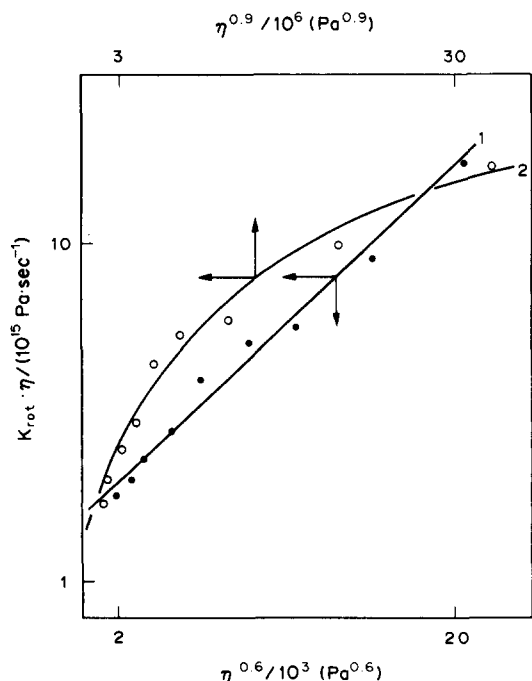


Fig. 5. Plots of experimental data for macroviscosity (η) and rotation rate constants (k_{rot}) of the MV probe in DGEBA corresponding to equation (5). 1, $\gamma = 0.6$; 2, $\gamma = 0.9$.

However, equation (14) is usable if $(\beta \cdot V_0)' \gg V_f'$. With the same fluorescence probe but different polymeric matrices, change in E_a^{rot} values indicates to a first approximation changes in V_f' values, because the $(\beta \cdot V_0)'$ factor is influenced mainly by the probe molecule. The mismatch of the probe and polymer structures in the glassy state creates a "hole" around the probe. Thus, it can be expected that, in glassy polymer states, the E_a^{rot} values are lower than those in elastic states.

The stated expressions allow calculation of the fractional critical free volume by means of experimental data for η and τ_{rot} , and to compare the contributions of different processes to the overall rotational process. Furthermore, T_g values can be calculated.

Studies in DGEBA

In DGEBA, changes in the macroscopic viscosity are possible by varying the temperature. Thus, both temperature dependence of η and viscosity dependence of τ_{rot} can be measured. A plot of the experimental data corresponding to equation (7) (in logarithmic version) gives a linear relationship expressed by

$$\ln \eta = \frac{77,200}{RT} - 23.1. \quad (17)$$

Thus, for DGEBA the activation energy for a Stokes process is given by $E_a^{\text{st}} = 77.2 \text{ kJ} \cdot \text{mol}^{-1}$.

The measured data for τ_{rot} and η were put into equation (5) and values for α , γ and δ evaluated by least-squares fits varying in the range of 0–1. Two results of such procedures are shown in Fig. 5. As can be seen, with $\gamma = 0.6$ the required linear plot between the experimental data is obeyed. Therefore, it can be assumed that 60% of the probe rotation is influenced by Stokes processes and *ca* 40% by a free volume diffusion. This estimate is supported by the results of another plot. As shown in Fig. 6, the $\ln \tau_{\text{rot}}$ vs $\ln \eta$ plot is linear. The mathematical expression of such dependence is given by

$$\ln \tau_{\text{rot}} = x \ln \eta + C \quad (18)$$

or

$$\tau_{\text{rot}} = C\eta^x. \quad (19)$$

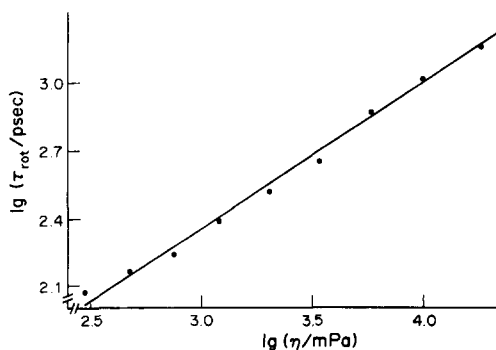


Fig. 6. Logarithmic plot for the dependence of the rotation lifetime (τ_{rot}) on macroviscosity (η) in DGEBA, corresponding to equation (18).

The exponent x has been calculated from Fig. 6 as 0.65. This value agrees with that of the above estimation. Further, other dyes possess similar x values, measured in other viscous media [31].

However, equation (19) is only linear over a small viscosity range (*ca* 10–5000 mPa) [32]. Thus, equation (5) is better suited for describing the situation over a wide range of η . The temperature dependence of τ_{rot} is given in Fig. 7. As expected, a linear relationship corresponding to equation (13) has been found and a value $E_a^{\text{rot}} = 44 \text{ kJ} \cdot \text{mol}^{-1}$ is obtained. Thus, the activation energy of the rotational process is only *ca* 60% of that of Stokes diffusion derived processes. As will be discussed below, the activation energy

$$\ln \tau_{\text{rot}} = \frac{44,000}{RT} - 21.6 \quad (20)$$

for probe rotation in polymer holes is very small. Therefore, in DGEBA the value 0.6 for the ratio E_a^{rot} to E_a^{dv} agrees well with the above evaluated γ exponent. Again, this result supports the assumptions that, also in the highly viscous diglycidylether investigated, some properties can be described with the free volume model. It is interesting to note that all modulated curves give approximately the same intercept. This result corresponds to the theoretical predictions.

Using equation (15), from the above experimental η/T relationship, the fractional free volumes V_f^* and V_f' can be calculated. T_g of glassy DGEBA was found to be -18°C . Using the experimental data, the following equation holds:

$$V_f' = 0.043 + 4.8 \cdot 10^{-4}(T - 255). \quad (21)$$

Thus, V_f' can be calculated for each temperature and, using equation (12), a plot of $\ln(\tau_{\text{rot}})$ against $1/V_f'$ is possible (Fig. 8). From the slope of this linear relationship, $(\beta V_0)'$ was found to be 0.55. At room temperature, the fractional free volume V_f' of DGEBA is 0.058. So, the requirement for use of equation (16) is satisfied.

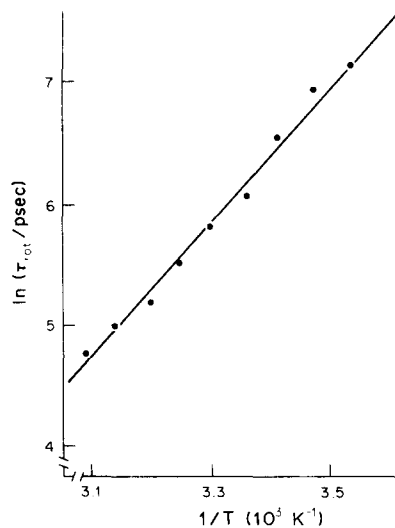


Fig. 7. Temperature dependence of rotation lifetime (τ_{rot}) in DGEBA corresponding to equation (13).

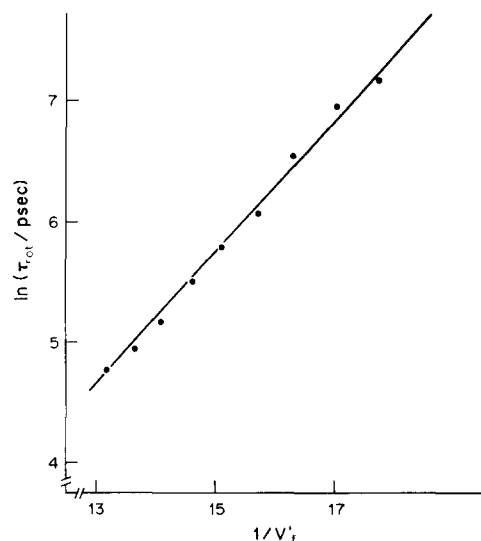


Fig. 8. Rotation lifetime τ_{rot} vs fractional free volume V_f' for the data on DGEBA.

The theoretical derivations require the plots corresponding to equations (10) and (13) must lead to the same τ_{rot}^0 value. For MV, with the experimental results of this paper, $\tau_{\text{rot}}^0 = 2.0 \text{ psec}$ [equation (10)] and $\tau_{\text{rot}}^0 = 1.5 \text{ psec}$ [equation (13)] have been obtained. These values agree quite well and lie in the expected regions.

Studies on the novolacs

In bisphenol-A derived novolacs (DNL), the fluorescence of MV decays according to bi-exponential curves, i.e.

$$I_f(t) = A_1 \exp(-t/\tau_f^1) + A_2 \exp(-t/\tau_f^2). \quad (22)$$

As for the mono-exponential decay, the different lifetimes (τ_f^1 and τ_f^2) were calculated by an iterative convolution procedure. As can be seen from the data summarized in Table 1, the τ_f^1 and τ_f^2 values differ markedly. Furthermore, the coefficients A_1 and A_2 , which indicate the proportions of the processes on the overall fluorescence, are very different. The short-lived excited state (τ_f^1) strongly dominates. But, both excited species responsible for the τ_f^1 and τ_f^2 processes refer to the MV molecule as shown by the emission spectra.

So far, the reason for the bi-exponential decay is unclear. Two explanations might be made:

- (1) probe molecules are located in two regions with different possibilities for relaxation processes;

Table 1. Lifetimes (τ_f^1 and τ_f^2) and distribution factors (A_1 and A_2) of the two emitting species of MV in novolac DNL 7.5

Temperature (C)	τ_f^1 (psec)	A_1	τ_f^2 (psec)	A_2
10	526	250	3400	9
15	518	250	4500	6
20	480	270	5500	4
30	470	270	4900	6
40	430	280	4500	5
50	390	300	5500	4
60	355	320	9500	4
70	313	340	20,000	4

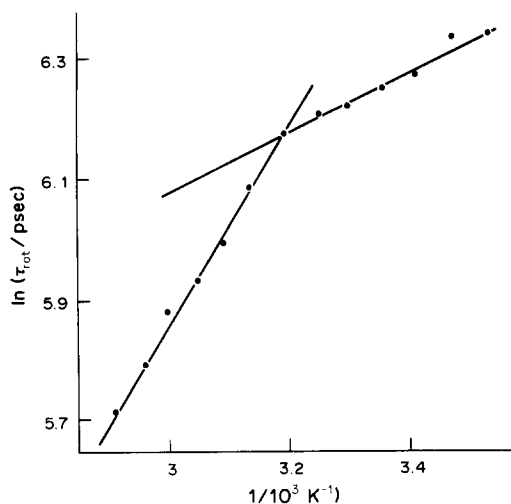


Fig. 9. Arrhenius plot for rotation lifetime (τ_{rot}) in DNL 7.5 corresponding to equation (13).

- (2) inhomogeneous distribution of the probe molecule in the matrix; a sum of exponential curves might occur but the bi-exponential decay describes best the fluorescence process.

These explanations are still speculative. For further discussion, only the τ_f^\dagger values are used. So, the main deactivation pathway of excited fluorescence probe has been monitored.

The Arrhenius plots of τ_f^\dagger values show a discontinuity (see Fig. 9). The crossing points of the two lines agree quite well with the T_g values found by DSC; data are listed in Table 2. Further, activation energies E_a^{rot} below and above T_g were calculated from the Arrhenius plots and are reported in Table 2.

As follows from these values, in the rubbery state of the novolacs ($T > T_g$), E_a^{rot} values are higher than those in the glassy state. Due to the higher microviscosity above T_g , the rotational process (k_{rot}) is more restricted and therefore more temperature-dependent. In the glassy state of the novolacs, the polymer chain movement is nearly frozen and the rotational process takes place mainly in "holes" of the polymeric matrix, resulting in smaller E_a^{rot} values.

Surprisingly, the different novolacs possess the same T_g . Probably, the investigated novolacs appear to be mixtures of bisphenol-A and oligomers. With HPLC techniques, in all DNL substances, the initial phenolic compound was detected. Such mixtures could be the reason for the almost constant τ_f^\dagger and T_g values observed in spite of a significant increase of

Table 3. Activation energies of probe rotational process (E_a^{rot}) and lifetimes of excited probe molecules at 20°C (τ_f) in DGEBA–novolac mixtures

Novolac	DGEBA content (mass %)	E_a^{rot} (kJ · mol ⁻¹)	τ_f (psec)
Without	100	44	640
DNL-5	95	42	790
DNL-5	73	40	1110
DNL-5	63	40	1650
DNL-5	58	37	1810
DNL-5	55	36	1950
DNL-5	0	14	359
DNL-7.5	55	31	1940
DNL-10	55	33	1880
DNL-12.5	55	33	2110
DNL-15	55	33	2110

\bar{M}_n . A similar result has been found for the lifetimes τ_f^\dagger (see Table 2).

Studies on DGEBA–DNL mixtures

To obtain information about initial non-hardened epoxy systems, mixtures of DNL and DGEBA have been investigated with the fluorescence probe MV. In such mixtures (mass contents of DGEBA see Table 3), only one emitting species was detected. Further, the logarithmic τ_{rot} values depend linearly on (temperature)⁻¹ corresponding to equation (13). Thus, within the temperature range investigated (10–70°C), no changes in the state of the polymeric system occur. As the E_a^{rot} values also indicate, the mixtures are in a viscous state for above T_g .

Results of τ_f and E_a^{rot} measurements for several DGEBA–DNL mixtures are listed in Table 3. As can be seen, with increasing content of DNL in the mixtures, the mobility of MV is reduced. Both the increased τ_f values and the decreased E_a^{rot} values support this statement. Probably, a stronger hydrogen-bond interaction between DNL and MV mainly causes the restricted mobility. In pure DNL however, the τ_f data do not correspond with that view. Perhaps the morphologies of the two systems are quite different. So, for geometrical reasons, hydrogen-bonds to the probe molecules are hindered. Again, the DNL type has less influence on the mobility data. Altogether, in DGEBA–DNL mixtures, evidence for strong hydrogen bonds between the components has been found using time-resolved fluorescence measurements. Such a situation must change the conditions for the curing process between the diglycidyl ether and novolacs. Indeed, the activation energy for that process (*ca* 80 kJ · mol⁻¹) is much higher than for the amine curing of epoxies (between 50–55 kJ · mol⁻¹). We will report more results on this process in the future.

Table 2. Average molar weights of the novolacs used (\bar{M}_n), fluorescence lifetime of the probe at 20°C, glass transition temperatures of the novolacs determined by fluorescence [T_g (f)], glass transition temperatures of the novolacs determined by DSC [T_g (DSC)], and activation energies of the probe rotation in the novolacs at $T > T_g$ [$E_a^{rot}(1)$] and at $T < T_g$ [$E_a^{rot}(2)$]

Novolac	\bar{M}_n (g/mol)	τ_f^\dagger (psec)	T_g (DSC) (°C)	T_g (f) (°C)	$E_a^{rot}(1)$ (kJ · mol ⁻¹)	$E_a^{rot}(2)$ (kJ · mol ⁻¹)
DNL-5	377	530	29	43	14 ± 3	3 ± 1
DNL-7.5	587	480	30	43	9 ± 2	4 ± 1
DNL-10	621	350	30	43	10 ± 2	3 ± 1
DNL-12.5	647	570	34	44	10 ± 2	5 ± 1
DNL-15	816	480	35	44	7 ± 2	3 ± 1

Acknowledgement—For determination of molecular weights and glass transition temperatures, we thank Dr K.-F. Arndt.

REFERENCES

1. V. Strehmel, L. Krukowka and M. Fedtke. *Chem. Techn.* **42**, 416 (1990).
2. R. G. Schmidt and J. P. Bell. *Adv. Polym. Sci.* **75**, 33 (1986).
3. C. Dumschat, H. Müller, H. Rautschek, H.-J. Timpe, W. Hoffmann, M. T. Pham and J. Hüller. *Sensors Actuators B* **2**, 271 (1990).
4. H.-J. Timpe, H. Baumann, C. Müller, H. Rautschek and M. Rautschek. *Chem. Techn.* **40**, 327 (1988).
5. H. Itagaki, K. Horie and I. Mita. *Prog. Polym. Sci.* **15**, 361 (1990).
6. J. Guillet. *Polymer Photophysics and Photochemistry*. Cambridge University Press, Cambridge (1987).
7. N. S. Allen and J. F. Rabek. *New Trends in the Photochemistry of Polymers*. Elsevier Applied Science, London (1985).
8. D. Phillips. *Polymer Photophysics-Luminescence, Energy Migration and Molecular Motion in Synthetic Polymers*. Cambridge University Press, Cambridge (1985).
9. R. L. Levy and S. D. Schwab. *ACS Symp. Ser.* **367**, 113 (1988).
10. M. Shmorhim, A. M. Jamieson and R. Simba. *Polymer* **31**, 812 (1990).
11. C. Noël, F. Laupetpre, C. Friedrich, C. Leonard, J. L. Halary and L. Monnerie. *Macromolecules* **19**, 201 (1986).
12. S. F. Scarlata and J. A. Ors. *Polym. Commun.* **27**, 41 (1986).
13. H.-J. Timpe, F. W. Müller, B. Strehmel, G. Panzner, K. Schiller and H. Reuter. *Angew. Makromolek. Chem.* (Submitted).
14. M. Kilches. Diplom Thesis. Technical University Merseburg (1990).
15. Landoldt-Börnstein. *Zahlenwerte und Funktionen aus Physik, Chemie, Astronomie, Geophysik und Technik*, 6th edn, Vol. V.
16. W. Rettig. *Angew. Chem.* **98**, 169 (1986).
17. M. Vogel and W. Rettig. *Ber. Bunsenges. Phys. Chem.* **89**, 962 (1985).
18. R. O. Loutfy. *Macromolecules* **14**, 270 (1981).
19. D. Anwand, F. W. Müller, B. Strehmel and K. Schiller. *Makromolek. Chem.* **192**, 1981 (1991).
20. B. Strehmel. Unpublished results.
21. C. D. Eisenbach. *Makromolek. Chem.* **179**, 2489 (1978).
22. W. C. Yu. *Macromolecules* **21**, 355 (1988).
23. H. Rau. *Photochromism—Molecules and Systems* (edited by H. Dürr and M. Bouas-Laurent), p. 16. Elsevier, Amsterdam (1990).
24. G. Stokes. *Trans Cambridge Phil. Soc.* **9**, 5 (1956).
25. S. Glasstone, K. J. Laidler and H. Eyring. *The Theory of Rate of Processes*, Chap. 9. McGraw-Hill, New York (1941).
26. A. Gierer and K. Wirtz. *Z. Naturforsch.* **89**, 532 (1953).
27. M. Vogel and W. Rettig. *Ber. Bunsenges. Phys. Chem.* **91**, 1241 (1987).
28. A. K. Doolittle. *J. appl. Phys.* **23**, 236 (1952).
29. M. Williams, R. F. Landel and J. D. Ferry. *J. Am. chem. Soc.* **77**, 3701 (1955).
30. A. K. Schulz. *J. Chim. Phys.* **51**, 530 (1954).
31. R. O. Loutfy and B. A. Arnold. *J. Phys. Chem.* **86**, 4205 (1982).
32. T. Förster and G. Hoffmann. *Z. Phys. Chem. (N.F.)* **75**, 63 (1971).